Uncertainty Quantification Employing a Streamline-Based Proxy for Reservoir Flow Simulation

A. R. Kovscek *, Y. Wang [1]

Department of Petroleum Engineering, Stanford University, Stanford, CA 94305-2220 U.S.A

Abstract

Carbon dioxide (CO_2) is already injected into a limited class of reservoirs for oil-recovery purposes; however, the engineering design question for simultaneous oil recovery and storage of anthropogenic CO_2 is significantly different from that of oil recovery alone. Currently, the volumes of CO_2 injected solely for oil recovery are minimized due to the purchase cost of CO_2. If and when CO_2 emissions to the atmosphere are managed, it will be necessary to maximize simultaneously both economic oil recovery and the volumes of CO_2 emplaced in oil reservoirs. This process is coined "cooptimization".

This paper proposes a workflow for cooptimization of oil recovery and geologic CO_2 storage. An important component of the workflow is the assessment of uncertainty in predictions of performance. Typical methods for quantifying uncertainty employ exhaustive flow simulation of multiple stochastic realizations of the geologic architecture of a reservoir. Such approaches are computationally intensive and thereby time consuming. An analytic streamline-based proxy for full reservoir simulation is proposed and tested. Streamline trajectories represent the three-

dimensional velocity field during multiphase flow in porous media and so are useful for quantifying the similarity and differences among various reservoir models. The proxy allows rational selection of a representative subset of equiprobable reservoir models that encompass uncertainty with respect to true reservoir geology. The streamline approach is demonstrated to be thorough and rapid.

Key words: CO_2 sequestration, streamlines, geological uncertainty, reservoir simulation

1 Introduction

Predictions of the mix of future primary energy sources often include significant use of fossil fuels and concomitant production of carbon dioxide (CO_2) from combustion. Moreover, scenarios envisioning a switch to renewable and/or nuclear primary energy sources rely on fossil fuels for the extended time period required to install large-scale systems. Despite the fact that other gases, such as methane and nitrous oxide, contribute to the greenhouse effect, experts project that CO_2 may account for about two thirds of potential global warming [1]. The magnitude of temperature response from increased atmospheric concentration of CO_2 is still being debated, but it may be wise to seek methods that allow continued use of fossil fuels while decreasing CO_2 emissions to the atmosphere. Such methods include increased energy conversion efficiency, conservation, utilization of low CO_2 producing fuels such as natural gas, and

* Corresponding author
Email addresses: kovscek@pangea.stanford.edu (A. R. Kovscek),
YWang18@slb.com (Y. Wang).
[1] Present address: Schlumberger, 4900 California Ave, 401A, Bakersfield, CA 93309

sequestration of CO_2.

Sequestration is the capture and long-term storage such that anthropogenic CO_2 is removed from the atmosphere for a significant, perhaps geologic, period of time [2]. One sequestration option is the injection of CO_2 into geologic formations including oil and gas reservoirs, deep unmineable coalbeds, and deep saline aquifers. First attempts at sequestration, the Sleipner project [3] withstanding, will likely be concentrated in the area of injection into sedimentary basins containing oil and/or gas. Oil and gas reservoirs have proven that they are effective at trapping fluids by the very fact that hydrocarbons accumulated. Moreover, enhanced oil recovery (EOR) efforts have used CO_2 since the 1970's; thus, regulatory and physical infrastructure already exists that can be adapted to CO_2 distribution and storage. Nevertheless, CO_2 storage in oil reservoirs is not a straightforward transfer of fossil fuel production technology, as others have suggested [4]. Consider that among other factors, considerable engineering effort has been directed toward minimizing the amount of CO_2 needed to recover a barrel of oil because the purchase cost of CO_2 is directly related to profitability. On the other hand, when the objective of CO_2 injection is to increase the amount of CO_2 left behind at the end of the recovery process, the approach to the design question changes considerably. We refer to the simultaneous production of oil and maximization of the volume of CO_2 in place as cooptimization.

The purpose of this paper and its successor [5] is to explore rigorously cooptimization and the workflow that allows it to be achieved. We do so by creating a 3D, geostatistical model of an oil reservoir based upon an actual field. The description of heterogeneities and their distribution is geostatistical in that multiple equiprobable reservoir models are generated capturing variabil-

ity and uncertainty. Uncertainty assessment is necessary because the future injection/production performance of oil and gas reservoirs cannot be predicted exactly. Further, the description of the fluids within the reservoir is compositional and realistic. This allows us to explore the important topic of miscibility of CO_2 in crude oil. Interestingly, this synthetic reservoir does not pass conventional screening criteria for CO_2 injection [6]. The oil is relatively viscous and dense. Consequently, CO_2 and the crude oil are not mutually soluble at pressures that are attained in the reservoir. Various scenarios are considered via numerical reservoir simulation to understand better reservoir development techniques that maximize the simultaneous production of oil and storage of CO_2 [5].

This paper specifically addresses the workflow used to accomplish cooptimization. A streamline derived proxy for full reservoir simulation is developed so that a subset of reservoir models encompassing our uncertainty regarding the true geology of a reservoir is selected rapidly and rationally. The subset of models is shown to span the range of possible flow behavior. It is upon this subset that computationally expensive flow simulations are conducted. This paper is organized accordingly: stochastic description of the synthetic reservoir, streamline proxy for comprehensive reservoir flow simulation, cooptimization workflow, uncertainty quantification employing the streamline-based proxy, discussion, and conclusions. Before embarking on these topics, relevant reservoir engineering concepts are reviewed. The properties of streamlines are reviewed at the same stage as the development of the streamline proxy.

2 Preliminaries

Injection of CO_2 into an oil reservoir increases ultimate oil recovery, and it is classified as an EOR (enhanced oil recovery) or tertiary displacement process [7]. At sufficient pressure, CO_2 is substantially soluble in the oil phase causing it to swell. Similarly, the injected CO_2 extracts components from the oil phase and transports them forward. Repetition of the extraction of crude-oil fractions and transport leads to miscibility of CO_2 in the crude oil, if pressure is sufficiently large. This is referred to as multi-contact miscibility [8]. And, the lowest pressure where miscibility develops is referred to as the minimum miscibility pressure (MMP). Miscibility is easiest to achieve at substantial pressure (order 10 MPa) in light or medium gravity oils (density less than 880 kg/m^3). The advantage of miscibility is that the microscopic, or pore level, displacement efficiency approaches 100 % [8]. At lower pressure and for more dense oil, CO_2 is not miscible in crude oil, and the recovery process is classified as immiscible CO_2 displacement.

An important parameter in any displacement process is the mobility ratio, M. During multiphase flow, the mobility of any phase within a porous medium is proportional to the effective permeability of the medium to the phase and inversely proportional to the viscosity of the phase. Phases with a small viscosity relative to other phases are highly mobile. The mobility ratio measures the mobility of the injected phase relative to that of the original oil phase. When M is greater than 1, the displacement is said to be unstable because the injected phase is more mobile than oil and channels selectively through the oil. The greater the value of mobility ratio, the more likely it is that preferential flow occurs. In such a case, the microscopic (i.e., pore-level) displacement effi-

ciency may be high, but the macroscopic storage efficiency is reduced through the combination of heterogeneity, high mobility ratio, and gravity segregation. These ideas are explored more fully elsewhere [9]. The endpoint mobility ratio quantifies the ratio of phase mobilities when each phase is at its greatest mobility. Throughout, we use mobility ratio and endpoint mobility ratio synonymously.

By way of clarification, the absolute permeability is a porous medium property that measures the ability of the porous medium to transmit fluid. It is determined by pore size and structure. When a single phase, such as gas or water, saturates the pore space of a rock, the absolute permeability determines the mobility of the phase. On the other hand, when two or more phases are present in the pore space of a rock, each phase is described by its own effective permeability. Generally, the sum of the phase effective permeabilities is less than the absolute permeability. Effective permeability increases or decreases as the fraction of the pore space occupied by a given phase increases or decreases. Relative permeability of a phase, k_r is the effective permeability divided by the absolute permeability.

During a reservoir injection process, it is customary to nondimensionalize time so that it is reported in pore volumes of fluid injected (PVI or PV). That is, the volume (at reservoir conditions) of fluid injected is divided by the void volume of the reservoir. The volume injected is obtained as the integral of injection rate with respect to time. Hence, 1 PV signifies that a volume equal to the volume of the reservoir has been injected.

In closing this brief review, we direct the non-petroleum engineer to a more thorough discussion of non-standard terminology in ref. [9].

3 Reservoir Description

A synthetic reservoir description is chosen that is based on an actual producing field. The PUNQ-S3 test case is described in detail elsewhere [10] and the geostatistical data is available electronically [11]. Briefly, the reservoir is dome shaped, bounded by faults, and underlain by an aquifer. Figure 1(a) displays the permeability field, where the (absolute rock) permeability is a quantitative measure of the conductivity of the rock to fluid. Dark shading indicates the most permeable portions of the reservoir. Fault location is called out by a thick dotted line. Figure 1(b) presents the porosity, or the void fraction of the rock. The most porous zones are darkly shaded. Figure 1 teaches that permeability and porosity are correlated positively. The ratio of average horizontal to vertical permeability is about 3.

The reservoir is composed of a series of fluvial sand and shale sequences with an average horizontal permeability on the order of 100 md (1 millidarcy (md) = 10^{-15} m^2) and a sand porosity of roughly 0.20. The correlation length varies with depth between 750 and 1500 m [12]. The distribution of the vertical permeability and horizontal permeability is approximated as log normal and simulated here with sequential Gaussian simulation [13]. This description is geostatistical in that numerous equiprobable realizations of the spatial distribution of permeability are readily obtained. Initial reservoir pressure is 25.3 MPa. Depth to the reservoir top is 2340 m. Mean reservoir thickness is 28 m.

Additionally, the reservoir pore volume is a relatively small 30 x10^6 m^3 (0.2 Bbbl), whereas the initial average oil saturation, S_o is 0.60. Saturation, S_i, is the fraction of the pore space filled with a given phase, i. If two or more phases

flow through the pore space of rock, each phase has its own so-called effective permeability. Relative permeability of a phase depends on the saturations of the various phases. The sum of all k_{ri} is always less than 1. The specific oil-water and gas-liquid two-phase relative permeability versus phase saturation, S_i relationships are shown in Fig. 2a and 2b, respectively. The symbols k_{rw}, k_{ro}, k_{rg}, k_{rog} denote water relative permeability in an oil-water system, oil relative permeability in an oil-water system, gas relative permeability in an gas-oil system, and oil relative permeability in gas-oil system, respectively. For calculation of three-phase relative permeability, the Stone II model is used [14]. The Stone model obtains relative permeability for the flow of three phases by interpolation among two-phase relative permeability data sets. The capillary pressure among oil, water, and gaseous phases is taken as 0.

Unfortunately, PUNQ-S3 does not have a compositional fluid description. A North Sea crude oil [15] is selected as the reservoir fluid because it exhibits properties similar to the black-oil description (oil formation volume factor, B_o, solution gas-oil ratio, R_s, and oil viscosity, μ_o, illustrated in Fig. 3) given with PUNQ-S3 [11]. Briefly, formation volume factor, Fig. 3a, is related to density and solution gas-oil ratio, Fig. 3b, describes gas solubility in oil. Because crude oils contain many components and may exhibit complicated phase behavior, the black-oil formulation is a simplified procedure to characterize crude-oil properties as a function of pressure. The formulation assumes that reservoir fluids are described by three components: oil, gas, and water. Pressure-volume-temperature properties of the fluids are assumed to be solely functions of pressure [15]. Whereas the black-oil formulation is sufficient for the simulation of some oil-recovery processes, such as water injection, it is too simple to describe CO_2 sequestration operations. Table 1 shows the compositional

description of the crude oil employed for calculations to follow and Fig. 3 the resulting black-oil properties that match those from the PUNQ-S3 data set. The crude oil density is 912 kg/m^3 (24^{o}API) and the oil viscosity, Fig. 3c, at reservoir conditions is about 2 mPa-s.

This reservoir and fluid combination is not prototypical for CO_2 enhanced oil recovery. The oil is relatively dense (i.e, heavy) and viscous. Consequently, the minimum miscibility pressure for pure CO_2 exceeds the maximum allowable reservoir pressure. That is, pure CO_2 is not completely miscible in the crude oil and displacement with pure CO_2 occurs in an immiscible fashion.

In this paper, we follow Barker et al [12] and discretize the reservoir into 19x28x5 (length x width x height) gridblocks. Each gridblock is 180 m^2 areally. The vertical dimension, from top to bottom, is discretized as 2.7, 4.8, 6.7, 6.7, and 6.7 m for layers 1 to 5, respectively. The ratio of horizontal to vertical permeability varies as 2.5, 4.0, 2.5 , 3.2, and 2.5 for each layer from top to bottom. We employ four producer and four injector wells as illustrated in Fig. 1. Arrows indicate that fluid is injected or withdrawn from a particular well.

The number and size of grid blocks affects simulation accuracy and the time required for computations. A grid refinement study reported elsewhere [16] employed simulation grids 4 and 16 times finer than that given above. The object of the grid refinement study was to verify that simulations on the grid above were subject to minimal numerical artifacts. Carbon dioxide and a miscible solvent gas were used as injectants. As the grid was made finer, oil recovery decreased by 1 and 3 % for the two injectants, respectively. The differences among results from the two finer grids were virtually undetectable. The original grid was judged to be sufficiently refined to yield accurate results.

In summary, our implementation does vary some from the original [10]. The number, type, and location of wells differs. We use a compositional fluid description. Also, the original gas-phase relative permeability was substituted with a curve more representative of gas injection in sandstones.

4 Streamline Proxy

Streamline and streamtube techniques are approximate methods for simulating fluid movement within reservoirs and aquifers [17–20]. Recently, they have undergone a renaissance [21–24]. They are most accurate when heterogeneity dominates the flow path and flow is incompressible or slightly compressible. A streamline is tangent everywhere to the instantaneous velocity field and, for symmetric permeability tensor, is normal to isobars or isopotential lines. Streamlines bound streamtubes that carry fixed volumetric flux. In three dimensions, flow rate is generally assigned to streamlines to avoid resolution of streamtube cross-sectional geometry [22,25]. The streamline method assumes that displacement along any streamline follows a one-dimensional solution and that there is no communication among streamlines. Thus, the three-dimensional flow problem is decomposed into a set of one-dimensional flow problems linked by common injection and production conditions. The time of flight (τ) of a particular streamline is the time required for a packet of fluid to transport from the origin to the end of a streamline. Streamline trajectories and τ are correlated with permeability distribution and reservoir structure; hence, they relate to reservoir performance. Unit mobility ratio ($M = 1$) streamlines are obtained analytically in one, two, or three dimensions and so are computed rapidly and efficiently.

Unit mobility ratio implies that the injected CO_2 is equally as mobile within the reservoir as the reservoir fluids. This is generally not the case because CO_2 is considerably less viscous than oil or water. Carbon dioxide is expected to be quite mobile. One might argue, therefore, that unit mobility ratio calculations are not representative of the true physics of flow; however, regions of the reservoir that are permeable (impermeable) have a large (small) density of streamlines that pass through them irrespective of M. Moreover, Wang and Kovscek demonstrated elsewhere [26,27] that unit and nonunit mobility ratio streamline calculations correspond in heterogeneous porous media. Under the assumptions of Dykstra and Parsons [28] for flow in heterogeneous and noncommunicating layered porous media and a large number of streamlines, they derived for any streamline that

$$\tau = \frac{M}{M-1}\left[1 - \left(1 + \tau'\left(\frac{1}{M^2} - 1\right)\right)^{\frac{1}{2}}\right] \tag{1}$$

where the superscript $'$ on τ represents the time of flight for unit mobility ratio, no superscript on τ represents any mobility ratio, and M is the endpoint mobility ratio. The implication of Eq. 1 is that the time of flight for nonunit mobility ratio results (i.e., nonanalytic) is related (in an approximate sense) to analytical unit mobility ratio time of flight.

4.1 Exhaustive Simulation Results

Before proceeding, we establish the correlation among comprehensive flow simulations and the corresponding analytical unit mobility ratio streamline calculations suggested above. For unit mobility ratio streamline computations, the simulator 3DSL [25] is used whereas for comprehensive flow simulation we

employ Eclipse [29]. Comprehensive flow simulation implies three-dimensional fluid transport incorporating gravity and compositional effects. The PUNQ-S3 "truth" case is taken as the true distribution of reservoir permeability and porosity. An additional, 1000 equiprobable reservoir models were generated using sequential Gaussian simulation [13]. Of these, Eclipse could run only 233 successfully.

There are numerous quantities that could be explored between unit mobility ratio streamlines and comprehensive flow simulation. Here, we illustrate three results: fluid produced upon tracer injected for simulation versus unit mobility ratio streamlines, oil produced upon water injected (M=2) for flow simulation versus unit mobility ratio streamlines, and CO_2 stored as predicted by compositional simulation versus unit mobility ratio streamlines. For both streamline and comprehensive flow simulation, the well conditions are set as producer bottomhole pressure equal to 120 bar and injector rates are 1000 m^3/day. Both water and gas injection are tested and compared because it is common to use alternating water and gas injection during CO_2 EOR.

Figure 4 presents the correlation among tracer injection results. In this case, straight-line relative permeability curves are input to the simulator; the viscosity and density of each phase is made equal. Each point on the figure represents the result from one model. Each axis plots the volume produced upon that injected after 1 pore volume (PV) of tracer has been injected. The numerical and analytical computations in Fig. 4 employ an identical physical description. The correlation coefficient is 0.97. This result serves to establish the effect of numerical errors, such as dispersion, in the finite-difference based comprehensive flow simulation. With no numerical error the correlation coefficient is 1, the slope of the line is 1, and the correlation passes through the

origin.

The comparison for a more realistic end-point mobility ratio of 2 (water is twice as mobile as oil) is illustrated in Figure 5. The initial average saturations (i.e., fraction of the pore space filled with a phase) of water and oil are 0.2 and 0.8, respectively. The fraction of produced fluid upon that injected is plotted for comprehensive flow simulation versus unit mobility ratio streamlines. Again, the total time corresponds to that required to inject a volume of water equal to the pore volume of the reservoir and a point represents the result from a single model. The correlation coefficient is about 0.80 and, as expected, somewhat less than that in Fig. 4. The results are scattered somewhat reflecting nonlinearities, such as gravity, and the nonunit mobility ratio, not incorporated in the analytical streamline computations. Nevertheless, correlation among unit mobility ratio streamlines and the comprehensive flow simulation is indicated.

A comparison was also made for the results of compositional CO_2 simulation versus the simple streamline calculation. Prior to CO_2 injection, the fraction of oil and water in the pore space are again 0.8 and 0.2. Although CO_2 is not fully miscible in the crude oil, a fraction of the injected CO_2 dissolves into the oil. This results in swelling and viscosity reduction of the oil phase. Figure 6(a) plots the fraction of CO_2 in place upon the total injected versus the same quantity from the analytical streamline computation. The correlation coefficient is 0.89 indicating strong correspondance among the simulations and analytical calculations. Figure 6b plots the mismatch, or difference, in this quantity from the realization taken as truth. The correlation coefficient is slightly lower, 0.83, and exhibits a fair degree of scatter. Nevertheless, Fig. 6(b) illustrates that a realization far from the truth produces a considerable mismatch when examined by a unit mobility ratio streamline flow computa-

tion. Models that are far from the truth case produce a large mismatch when computed from comprehensive flow simulation using true mobility or strictly from unit mobility ratio calculations.

Further tests of the streamline-based proxy were conducted. For instance, the ability of a streamline calculation to predict the breakthrough time calculated with comprehensive flow simulation correlated with a coefficient of 0.8. Similarly, unit mobility ratio streamlines versus first-contact miscible flow simulations for the volume of CO_2 in place demonstrated a correlation coefficient of 0.7. The results above make apparent that the streamline proxy is suitable for screening various realizations of reservoir geometry prior to full-physics compositional reservoir simulations.

5 Cooptimization Workflow

With the validity of unit mobility ratio streamline calculations as an approximate proxy for full-physics flow simulation established, a workflow for cooptimized CO_2 storage and oil recovery follows. The first step in a combined sequestration and oil recovery project is the location of possible sites for such a project. Previous publications [30,31] address screening criteria relevant to the CO_2 storage problem. In short, aspects including reservoir depth, storage capacity, water and oil volumes in place, formation thickness, and permeability need to be considered in concert. The density of CO_2 with depth alone is not a sufficient criterion for choosing candidate sites. It is necessary to consider porosity and the amount of oil and water that are displaceable.

Once a site has been identified, the workflow must assess the effect of uncer-

tainty on results from flow predictions, identify injection and recovery processes that achieve the combined optimum, and elucidate schemes that reduce cycling of injectant. A workflow for designing a combined sequestration and EOR process is

(1) Describe the reservoir incorporating uncertainty in the distribution of permeability.
(2) Quantify the magnitude of uncertainty with respect to flow prediction and CO_2 retention.
(3) Choose an appropriate injection gas composition. Economics dictate either maximization of the injected concentration of CO_2 or minimization of the purchase cost of injectant.
(4) Identify reservoir processes that jointly maximize oil production and the volume of CO_2 in place while minimizing the production and cycling of CO_2.
(5) Design well placement and completions to reduce the preferential flow of injected gas through high permeability zones.
(6) As required and as economics dictate, implement gas mobility control to increase the time required for the transport of injectants to a producer.

The first step is entirely within the realm of geostatistics. That is, the generation of realistic equally probable numerical reservoir models that honor geological information (mainly permeability measurements). This step is fulfilled here within section **3 Reservoir Description**. The second step acknowledges that significant uncertainty exists in the detailed distribution of reservoir properties, such as permeability, because the known data are relatively sparse. When flow simulation is performed on various realizations to predict performance, the uncertainty in geological description is transferred

to a relatively uncertain prediction of performance. The second step might be restated as choose a limited number of reservoir models for comprehensive flow simulation that yield significantly dissimilar results and span the range of uncertainty. The remaining steps get at the heart of the reservoir and production engineering design question for sequestration.

6 Uncertainty Quantification

Various methods of uncertainty estimation have been proposed, but appear to be either heuristic or require a comprehensive flow simulation for a large number of realizations of possible reservoir architecture. For instance, linear uncertainty analysis [32] and the scenario test method [33] perturb the reservoir model around a single supposedly most likely reservoir model. Additionally, multiple models can be generated and constrained to available data by geostatistical techniques [34]. Typically, these cases are pilot point methods. Values at sparse locations within the reservoir are adjusted and the changes propagated to the entire reservoir volume by the krigging interpolation procedure [13].

Among the simplest approaches is entirely stochastic. This approach is akin to a shotgun blast. A large number of realizations are used for comprehensive flow simulation generating voluminous data. An advantage is the wide range of behavior displayed and the relatively straightforward algorithm for obtaining the data. The approach however is time consuming. Multiple simulations are conducted that yield quite similar results.

Our approach is to use the properties of unit mobility ratio streamlines as a

proxy for full reservoir simulation. The proxy does not substitute for comprehensive simulation, but rather screens the full range of variability so that a representative suite of models is obtained that are then used for comprehensive flow simulation. Uncertainty quantification involves a number of stages:

(1) Start from a geostatistical reservoir model and generate a sufficiently large number of equiprobable realizations of the spatial distribution of reservoir properties such as permeability and porosity. If some reservoir production history is available, the reservoir model can be constrained by the dynamic data (e.g., [27,35]).
(2) Trace unit mobility ratio streamlines on each realization. Pollock's method [36] is used here.
(3) For each of the reservoir models considered, compute an appropriate output value such as the amount of CO_2 in place or the volume of oil produced after a given amount of injection.
(4) For the suite of models, compute the distribution (i.e., probability density function) resulting from a unit mobility ratio calculation. Thus, identify the most likely and outlier models. This approach allows fairly easy delineation of reservoir models for low, median, and high-side predictions.
(5) Perform comprehensive flow simulation on the subset of models to predict possible future performance as well as quantify the uncertainty of predictions.

A water injection and a CO_2 injection case are tested to demonstrate the methodology. The same 1000 equiprobable reservoir models are used again.

6.1 Water Injection

The reservoir simulator is run in "black-oil" mode to reduce run time. That is, there are oil, water, and gas components whose properties are a function of pressure only as illustrated in Fig. 3. Figure 7 illustrates the distribution of results obtained when the volume of oil produced upon the volume of water injected ($\frac{N_p}{N_j}$) at 1 PV of water injection is ranked using unit mobility ratio streamlines. Results from 1000 reservoir models are shown. From these 1000 streamline calculations, 21 reservoir models were selected that appear to span the most likely and outlier results. Comprehensive flow simulation was then conducted on these 21 models. As Fig. 7 shows, the distribution shifts to the right somewhat. Additionally, comprehensive flow simulation was performed on all 233 of the reservoir models that could execute on the simulator. Comparison of the results from the full-physics flow simulations shows that the sampling methodology well represents the distribution obtained from execution of the 233 models. The small sample size of 21 models does not reproduce the shape of the distribution near the maximum and minimum. Nevertheless, the mean and standard deviation of the 21 and 233 model sets are quite similar.

The computational effort was gauged via wall clock timings. All computations were conducted on a Dell Pentium PC containing a 2 GHz processor. The streamline calculations and sorting procedure completed in roughly 17 min. Another 17 min. were required to run the 21 models that were chosen as representative of uncertainty in the geological description. The exhaustive simulations (233 models) that were conducted to verify that sampling was indeed representative consumed 190 min. The speed-up factor is about 6. Recall

that problem complexity was reduced significantly by reducing oil to a single component as appropriate for water injection problems. Also, if a more finely gridded model was employed, the speed-up factor would be larger due to the greater computational requirements of the reservoir simulator.

6.2 CO_2 *Injection*

A similar procedure was repeated for pure CO_2 injection. Figure 8 shows the distribution of CO_2 stored as a fraction of that injected obtained from streamline calculations. From these results 8 models were chosen based on the volume of CO_2 in place ($\frac{N_s}{N_j}$) at about 1 PV of injected CO_2. Figure 8 also plots the frequency obtained using comprehensive flow simulation. The small sample size skews histogram reproduction ($1/8 = 0.125$). Nevertheless, it is clear that the models sampled span the range of variability in the full set of reservoir models.

These 8 models were examined for a variety of output. Figure 9 plots the instantaneous producing gas-oil as a function of time. Results from the truth model are also shown for each of the 4 producing wells. The predictions are varied, and the technique has allowed us to select efficiently these 8 models without the need to conduct tens or hundreds of comprehensive flow simulations. Note the predictions indicate that gas breakthrough should occur in less than 1000 days in virtually all cases. Additionally, Fig. 9 teaches that some form of mobility control is essential for this example reservoir. Otherwise, injectors and producers link up fairly rapidly and much gas is cycled through the reservoir. Reduction of gas cycling and mobility control are important topics for cooptimization in part 2 [5].

Again, wall clock timing was used to examine computational efficiency. The streamline ranking is identical to that for the water injection problem and so required 17 min. The 8 models chosen by the streamline ranking procedure required 140 min to run on the fully compositional, full- physics simulator. The exhaustive simulations conducted to verify the sampling methodology required 4194 min. to complete. The speed-up factor is about 27.

7 Discussion

There are several items that need to be discussed in greater detail. First, the correlation of unit mobility streamline computations with non-unit mobility ratio simulations is elaborated. Second, inaccuracy in the prior model for reservoir properties is discussed. Third, it is shown how one obtains a "best guess " estimate and how uncertainty in that guess is quantified. Lastly, implications are drawn out of this work for sequestration in saline aquifers.

Comparison of the correlation coefficients in Figs. 5 and 6 indicates that the correlation among unit-mobility ratio streamlines and simulation increases somewhat as the mobility ratio for displacement becomes more unfavorable (i.e.,larger). It is counterintuitive, at first, that less stable displacements correlate better with unit mobility ratio results. In geologic media, the spatial distribution of heterogeneity dominates displacement character and the effects of heterogeneity become more pronounced as mobility ratio increases. The strong coupling of the distribution of permeability with displacement behavior explains the excellent correlation for quite unstable displacements. Even though mobility ratio varies, the relative rank among reservoir models is maintained. A model that leads to retention of a large fraction of injected

CO_2 as indicated in an $M = 1$ calculation also yields a relatively large retained fraction for $M > 1$. Wang and Kovscek [27] explore this topic further in the context of streamline-based history matching.

Whereas the streamline computations do indicate some aspects of viscous fingering, they do not capture the effect of gravity. A gravity number is defined as

$$N_G = \frac{L^2 k_z \Delta\rho}{H k_h \Delta p} \tag{2}$$

where k is permeability, the subscripts z and h represent vertical and horizontal, respectively, L is the horizontal distance between injector and producer, H is the formation thickness, Δp is the pressure drop between injector and producer, and $\Delta\rho$ is the density difference between oil and the injected fluid. We performed several numerical experiments to gauge the effect of gravity on our ability to correlate streamline properties with the full flow physics. In the waterflood case above, the density of oil is 912 kg/m^3 and N_G is 0.7. When oil density increases to 1000 kg/m^3 so that it is the same as water, the correlation coefficient increased only 1 %. On the other hand, reducing the oil density to 750 kg/m^3 increases the gravity number to 2. The correlation coefficient only decreases by 1 % from the base case or 2 % from the no-gravity case. For pure CO_2, the injected phase is dense and supercritical. In fact, CO_2 density is relatively close to the oil density. Hence, not incorporating the effect of gravity in the streamline proxy has a measurable, but small, effect on the goodness of correlation.

The examples and method development presented here do not incorporate any dynamic data. As a result, Fig. 9 displays a rather substantial range of differ-

ence among the performance of the various models. Oil production and CO_2 storage display similar variability, although not shown. If a reference model exists (either constrained or unconstrained by geostatistical data) that has been established by history matching, then we may construct unit mobility ratio streamlines on the reference model and obtain the distribution of the time of flight of the various streamlines. Additional reservoir models consistent with the prior reservoir model are generated. Then models are selected based on their mismatch to the reference history matched model so that the selected models span a limited range of mismatch to the production history (cf, [27]). Future performance is then constrained by the prior and known history. Generally, incorporation of a greater volume of high-quality production data increases certainty.

Along a similar line of discussion, the prior reservoir model in all of the work here is identical to the true reservoir model. In reality, the prior model is known with less certainty because of measurement error and the relatively small sample size relative to the reservoir. The framework employed can just as efficiently examine uncertainty in the prior model. The prior model could be perturbed or changed entirely. For instance, instead of a Gaussian distribution of properties one might postulate that a bivariate or some other complicated distribution exists [37]. Unit mobility streamline calculations allow one to explore in a short period of time any plausible prior model. From this exploration of flow behavior and reservoir connectivity, a few realizations of reservoir architecture are chosen rationally to explore more fully the variability in predictions.

Continuing the theme of uncertainty quantification, we recall that the generation of reservoir models, such as Fig. 1, that lead to "upside", "most likely",

and "downside" prediction of reservoir performance is a fairly standard practice in the oil industry to grapple with uncertainty. These are sometimes referred to as "P90", "P50", and "P10" models reflecting where they lie on a cumulative density function. The various models, however, may be constructed in a heuristic fashion.

The streamline-based proxy gives a robust process to sample the posterior probability density function and locate reservoir models that can then be used to quantify more exactly the possible range of performance. For example, Fig. 8 illustrates that our "most-likely" prediction of the amount of CO_2 stored within the PUNQS3 reservoir is 0.37 PV and that the uncertainty in this prediction is about $\pm$ 0.07 PV. This is a variation of roughly 20 %. Part II of this work discusses how the fraction stored is increased and illustrates the variability of predictions [5].

A nontrivial extension of the unit-mobility streamline proxy is to aquifer sequestration of CO_2 where there are at least two domains of interest. The first is flow through the aquifer itself. The techniques above appear to be almost directly applicable to this domain. The second is the possible movement of CO_2 into the strata overlying the aquifer. The geologic media above the aquifer are likely to be poorly characterized, but it may be necessary to estimate the probability that CO_2 can reach the surface, and if so the transport time. Constant pressure boundaries are easily implemented at the surface as a row of production wells operating at constant pressure. During active injection, unit mobility streamlines can be constructed that teach whether various realizations differ greatly with respect to the transport time for CO_2 to the surface. In this way, a wide range of variability in the geologic structure can be probed. Of course, comprehensive flow simulations including the effects of

gravity and dissolution of CO_2 in brine are still needed for a suite of models to obtain accurate measurements. In short, the streamline methodology may allow rapid estimates of $\frac{N_{aquifer}}{N_j}$, where $N_{aquifer}$ is the volume of CO_2 held within the aquifer and $1 - \frac{N_{aquifer}}{N_j}$ is the volume lost to the strata above the aquifer.

8 Conclusion

Geologic data, especially when unconstrained by any dynamic information, is quite uncertain. It is appropriate to gauge and quantify uncertainty at the outset of the discussion of geologic sequestration of CO_2 where the aim is to reduce the emission of CO_2 to the atmosphere. The first steps in the workflow for sequestration are characterization of the reservoir and quantification of the uncertainty in the characterization with respect to flow results. To gauge uncertainty and predict future performance, it is necessary to select a set of reservoir models that span a range of possible reservoir performance. The most direct method of selection is to generate an appreciable number of equiprobable reservoir models, run comprehensive or full-physics flow simulations on these models, and rank the results. However, conducting full flow simulation on a large number of reservoir models is time consuming. The analysis of such data is also time consuming and perhaps adds little incremental benefit. Therefore, a proxy is developed that is computed rapidly and relates directly to the flow of fluids within a reservoir.

Unit mobility ratio streamlines correlate approximately with results from non-unit mobility ratio reservoir simulation. Streamlines provide important information about the connectivity, or lack thereof, among injectors and producers

and the distribution of heterogeneities within a reservoir. The process of defining the distribution of reservoir performance via comprehensive flow simulation is simplified by replacing it with sampling from the uniform distribution (rank) of unit mobility ratio streamline results.

Nomenclature and Abbreviations

B	formation volume factor, dimensionless
EOR	enhanced oil recovery
H	vertical reservoir thickness, m
k	absolute rock permeability, md, 1 md = $10^{-15}\mathrm{m}^2$
k_{ri}	relative permeability of phase i, dimensionless
L	shortest horizontal distance between injector and producer, m
M	endpoint mobility ratio, dimensionless
MMP	minimum miscibility pressure , bar or Pa
N	volume as a fraction of the total reservoir void or pore volume, dimensionless
N_G	gravity number, dimensionless
P	pressure, bar or Pa
PV	pore volume, pore volume injected, dimensionless
R_s	solution gas-oil ratio, dimensionless
S	phase saturation, dimensionless
T	temperature, ^{o}C or K

Greek

Δp	pressure difference, bar or Pa
$\Delta \rho$	density difference between oil and injected fluid, kg/m^3
τ	time of flight along a streamline, s

Subscripts and Superscripts

$'$	denotes time of flight calculated assuming that M=1
c	critical
g	gas phase
h	horizontal
j	injected
o	oil phase
og	two-phase system composed of oil and gas phases
p	produced
s	stored
w	water phase
z	vertical

Acknowledgement

Support was provided by the Assistant Secretary for Fossil Energy, Office of Coal and Power Systems, through the National Energy Technology Laboratory

and the GEO-SEQ project of the Lawrence Berkeley National Laboratory.

References

[1] Herzog, H., Eliasson, B, and Karstad, O. Capturing Greenhouse Gases, *Scientific American* 2000; **Feb**: 72–79.

[2] Reichle, D, Houghton, J, Benson, S et al. Working Paper on Carbon Sequestration Science and Technology, Office of Science, U.S. Department of Energy, 1999; http://www.doe.gov//.

[3] Korbol, R and Kaddour A. Sleipner West CO_2 Disposal–Injection of Removed CO_2 into the Utsira Formation, *Energy Convers. Mgmt*, 1999; **36(3-9)**: 509–512.

[4] Stevens, SH and Gale, J. Geologic CO2 Sequestration May Benefit Upstream Industry, *Oil and Gas J.*, 2000; **May 15**: 40-44.

[5] Cakici, MD and Kovscek, AR. Geologic Storage of Carbon Dioxide and Enhanced Oil Recovery II: Cooptimization of Storage and Recovery, *Energy Convers Mgmt*, submitted 2003.

[6] Taber, JJ, Martin, FD, and Seright, RS. EOR Screening Criteria RevisitedPart 1: Introduction to Screening Criteria and Enhanced Recovery Field Projects, *Soc. Pet. Eng. Res. Eng.*; 1997:**Aug**: 189-198.

[7] Kovscek, AR. Petroleum Recovery in *Encyclopedia of Petroleum Science & Engineering*, Speight J. G. Ed., New York: Marcel Dekker, to appear.

[8] Kovscek, AR. Immiscible Carbon Dioxide Displacement in *Encyclopedia of Petroleum Science & Engineering*, Speight J. G. Ed., New York: Marcel Dekker, to appear.

[9] Jessen, K, Kovscek, AR, and Orr, F M Jr. Increasing CO_2 s Storage in Oil Recovery, *Energy Convers Mgmt*, submitted 2003.

[10] Floris, FJT, Bush, MD, Cuypers, M. Roggero, F. and Syversveen AR. Methods for Quantifying the Uncertainty of Production Forecasts: A Comparitive Study, *Petrolem Geoscience*, 2001; **7** SI: S87-S96.

[11] TNO PUNQ-S3, http://www.nitg.tno.nl/punq/cases/index.shtml.

[12] Barker, JW, Cuypers, M., and Holden, L. Quantifying Uncertainty in Production Forecasts: Another Look at the PUNQ-S3 Problem, *Soc Pet Eng J*, 2001; **6(4)**: 433-441.

[13] Deutsch, CV and Journel AG. *GSLIB Geostatistical Software Library and User's Guide*, New York: Oxford University Press, 1992. p. 117–184.

[14] Stone, H. Estimation of Three-Phase Relative Permeability and Residual Oil Data, *J Can Pet Tech*, 1973; **Oct-Dec**: 53-61.

[15] Pedersen, KS, Fredenslund, Aa, and Thomassen, P. Table 4-4, *Properties of Oils and Natural Gases*, Houston, Gulf Publishing Co., 1989. p. 72.

[16] Cakici, M. D. *Co-Optimization of Oil Recovery and Carbon Dioxide Storage*, Engineer Thesis, Stanford University, December 2003.

[17] Higgins, RV and Leighton, AJ. A Computer Method to Calculate Two-Phase Flow in Any Irregularly Bounded Porous Medium, *J Pet Tech*, 1962; **June**: 679-683.

[18] Higgins, RV, Boley, DW, and Leighton, AJ. Aids to Forecasting the Performance of Water Floods, *J Pet Tech*, 1964; **Sept**: 1076-1082.

[19] Martin, JC and Wegner, RE. Numerical Solution of Multiphase, Two-Dimensional Incompressible Flow Using Streamtube Relationships, *Soc Pet Eng J*, 1979; **Oct**: 313-323.

[20] Fay, CH and Prats, M. The Application of Numerical Methods to Cycling and Flooding Problems. in *Proceedings of the 3rd World Petroleum Congress*, 1951.

[21] Hewett, TA and Behrens, RA. Scaling Laws in reservoir Simulation and Their Use in a Hybrid Finite Difference/Streamtube Approach to Simulation the Effects of Permeability Heterogeneity, in *Reservoir Characterization, II* , L. Lake and H.B.J. Carroll (eds.), London: Academic Press Inc., 1991. p. 402-441.

[22] Thiele, MR, Batycky, RP, Blunt, MJ, and Orr Jr, F.M Jr. Simulating Flow in Heterogeneous Systems Using Streamtubes and Streamlines, *Soc Pet Eng Res Eng*, 1996; **Feb**: 5-12.

[23] King, MJ. and Datta-Gupta, A. Streamline Simulation: A Current Perspective, *In Situ*, 1998; **22(1)**: 91-140.

[24] Blunt, MJ, Liu, K, and Thiele, MR. A Generalized Streamline Method to Predict Reservoir Flow, *Petroleum Geoscience*, 1996; **2**: 259-269.

[25] Batycky, RP, Blunt, MJ, and Thiele, MR. A 3D Field-Scale Streamline-Based Reservoir Simulator, *Soc Pet Eng Res Eng*, 1997; **Nov**: 246-254.

[26] Wang, Y and Kovscek, AR. Streamline Approach for History Matching Production Data, *Soc Pet Eng J*, 2000; **25**: 353-362.

[27] Wang, Y and Kovscek, AR. Integrating Production History into Reservoir Models Using Streamline-Based Time-of-Flight Ranking, *Petroleum Geoscience*, 2003; **9(2)**: 163-174.

[28] Dykstra, H and Parsons, RL. The Prediction of Oil Recovery by Waterflood, In *Secondary Recovery of Oil in the United States, Principles and Practice*, 2d ed., New York: American Petroleum Institute, 1950. p. 160-174.

[29] GEOQUEST, ECLIPSE User's Manual, Schlumberger Information Systems, 2002.

[30] Kovscek AR. Screening Criteria for CO_2 Storage in Oil Reservoirs, *Petroleum Science and Technology* 2002; **20(7&8)**: 841–866.

[31] Bachu S. Sequestration of CO_2 in geological media in response to climate change: road map for site selection using the transform of the geological space into the CO_2 phase space, *Energy Conversion and Management* 2002; **43**:87-102.

[32] Lepine, OJ, Bissell, RC, Aanonsen, SI, Pallister, I and Barker, JW. Uncertainty Analysis in Predictive Reservoir Simulation Using Gradient Information, *Soc Pet Eng J*, 1999; **5(4)**: 251–259.

[33] Rogerro, F. Direct Selection of Stochastic Model Realizations Constrained to Historical Data, paper SPE 38731 presented at the 1997 SPE Annual Technical Conference and Exhibition, San Antonio, TX 5-8 Oct.

[34] Wen, XH, Clayton, DV, and Cullick AS. High Resolution Reservoir Models Integrating Multiple-Well Production Data, *Soc Pet Eng J*, 1998; **4(4)**: 344–355.

[35] Caers, J, Krishnan, S, Wang, Y, and Kovscek, AR. A Geostatistical Approach to Streamline-Based History Matching, *Soc Pet Eng J*, 2002; **7(3)**: 250–266.

[36] Pollock, DW. Semianalytical Computation of Path Lines for Finite-Difference Models *Ground Water*, 1998; **26(6)**: 743-750.

[37] Strebelle, S. Conditional Simulation of Complex Geological Structures Using Multiple-Point Statistics, *Mathematical Geology*, 2001; **34(1)**: 1-22.

Table 1

Compositional description of crude oil.

Component	Mole fraction	Molecular weight kg/mol	T_c (K)	P_c (bar)	Accentric factor
carbon dioxide, CO_2	0	0.04401	304.2	72.9	0.228
methane, CH_4	0.4383	0.01604	190.6	45.4	0.008
ethane, C_2H_6	0.04262	0.03007	305.4	48.2	0.098
propane, C_3H_8	0.009153	0.04410	369.8	41.9	0.152
i-butane, C_4H_10	0.005824	0.05812	408.1	36.0	0.176
n-butane, C_4H_10	0.005395	0.05812	425.2	37.5	0.193
i-pentane, C_5H_12	0.006771	0.07215	460.4	33.4	0.227
n-pentane, C_5H_12	0.003081	0.07215	469.6	33.3	0.251
hexanes, C_6	0.01063	0.08617	507.4	29.3	0.296
heptanes, C_7	0.2359	0.1355	623.9	30.4	0.449
$C_8 - C_{15}$	0.1189	0.2489	708.6	20.4	0.804
$C_{16} - C_{23}$	0.07894	0.3812	795.7	16.5	1.119
$C_{24}+$	0.04456	0.6322	947.9	14.5	1.317

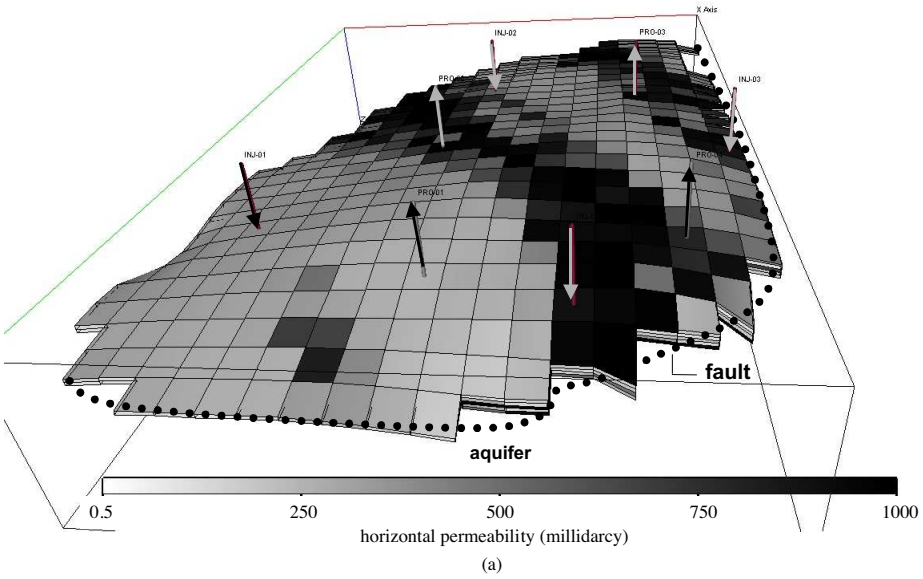

(a)

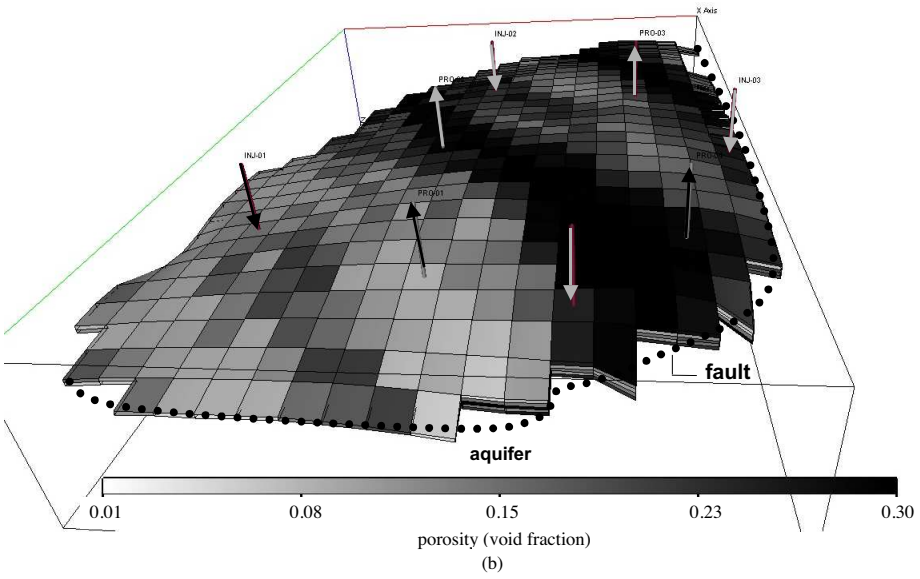

(b)

Fig. 1. Truth case reservoir architecture: (a) distribution of horizontal permeability (md) and (b) distribution of porosity (fraction). Arrows indicate location of injection (downward) and production (upward) wells.

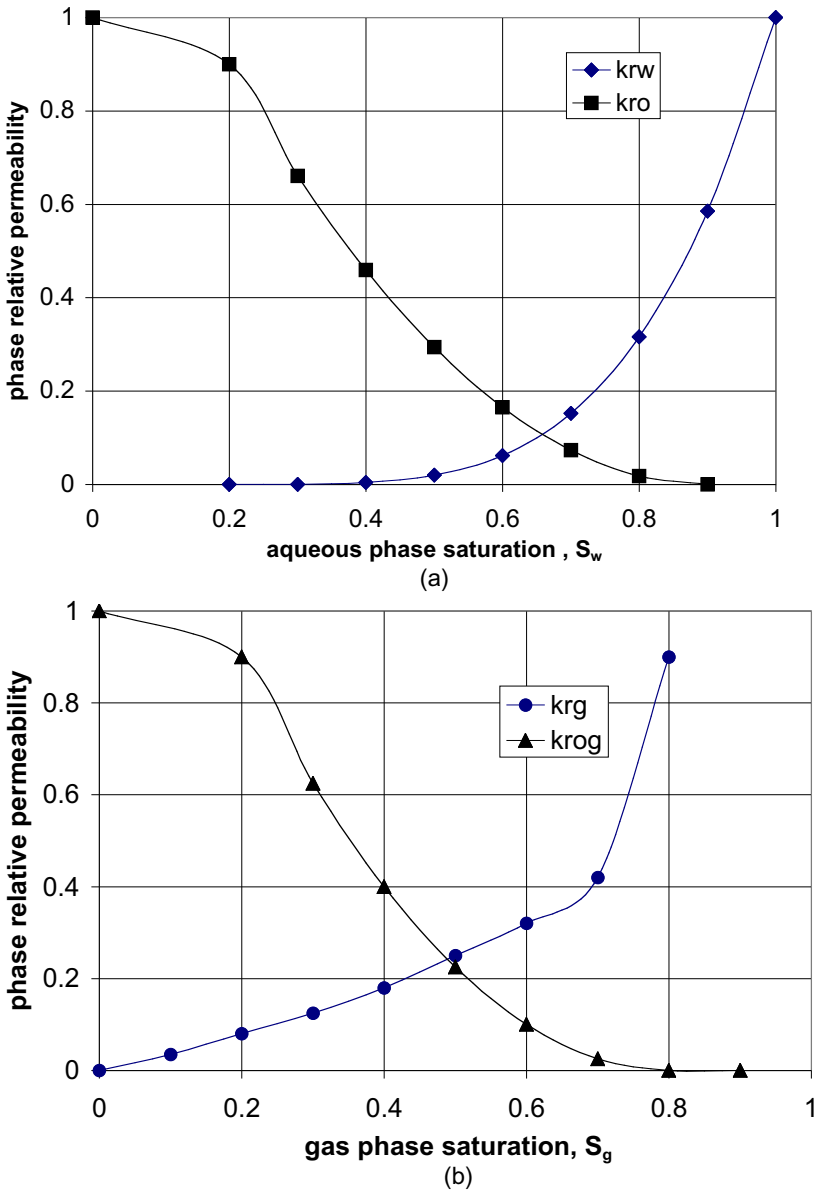

Fig. 2. Two-phase relative permeability relationships: (a) water and oil and (b) oil and gas.

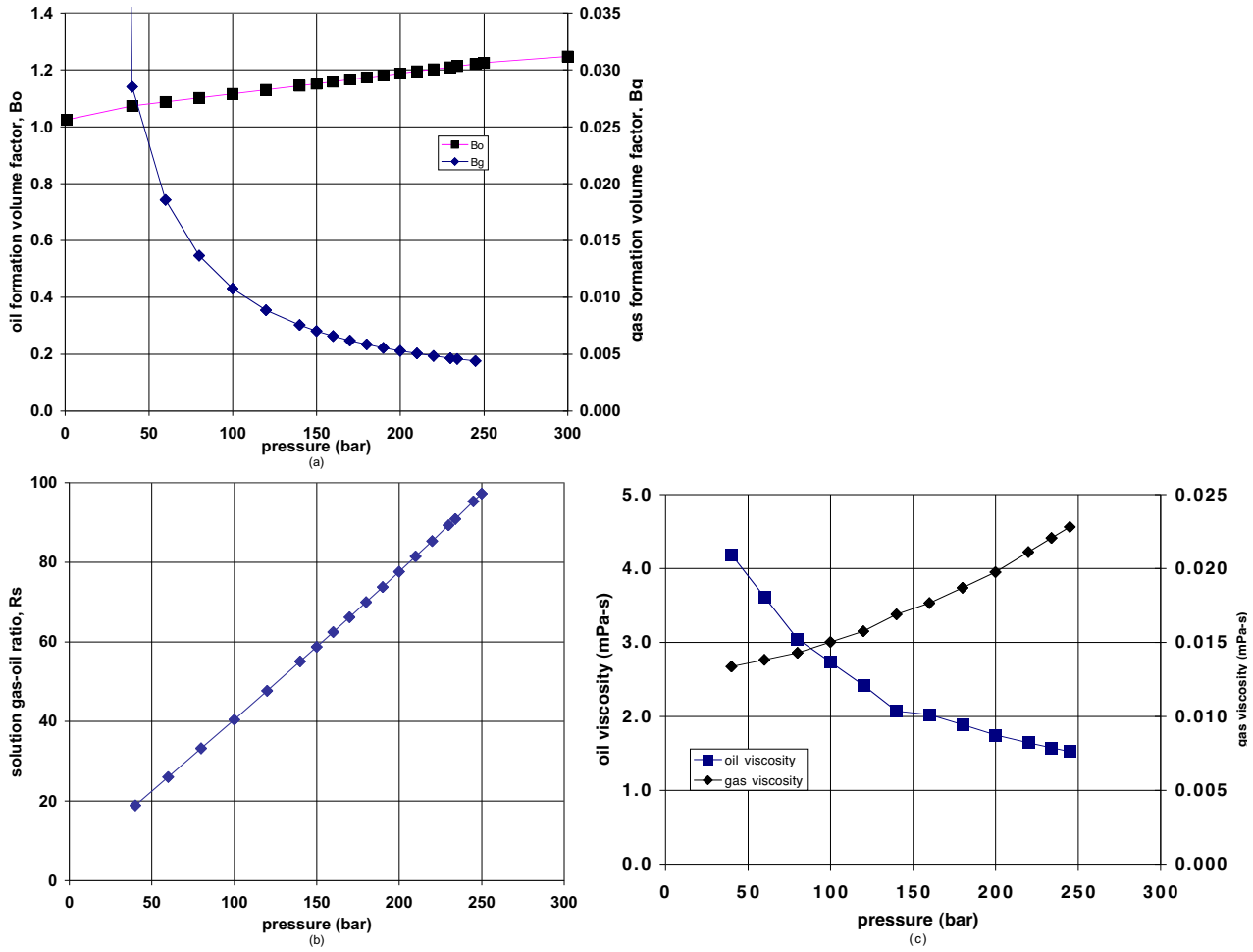

Fig. 3. Black-oil pressure-volume-temperature properties of reservoir fluids: (a) oil and gas formation volume factors versus pressure, (b) solution gas-oil ratio versus pressure oil, and (c) gas viscosity versus pressure.

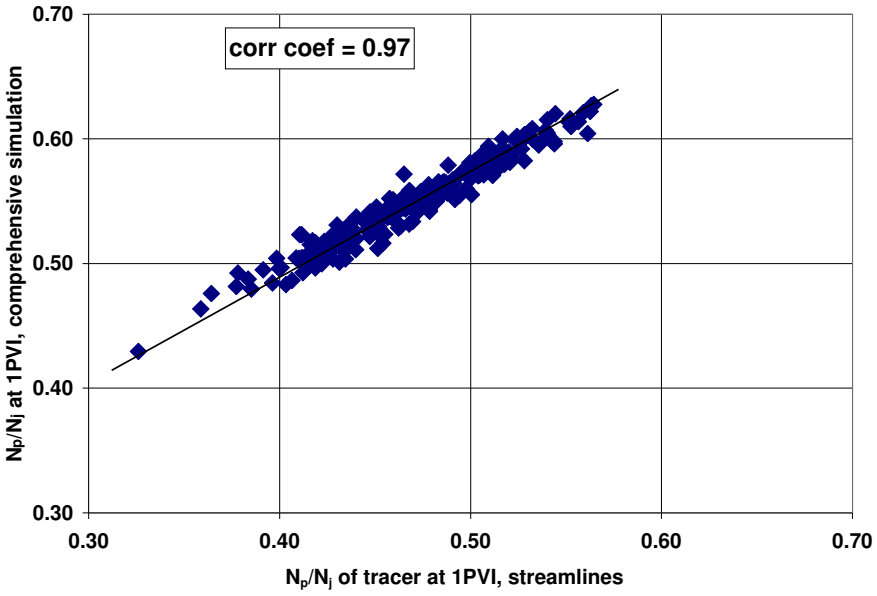

Fig. 4. Correlation among streamline and simulation results. The volume of tracer produced upon the total tracer injected is plotted at 1 PVI.

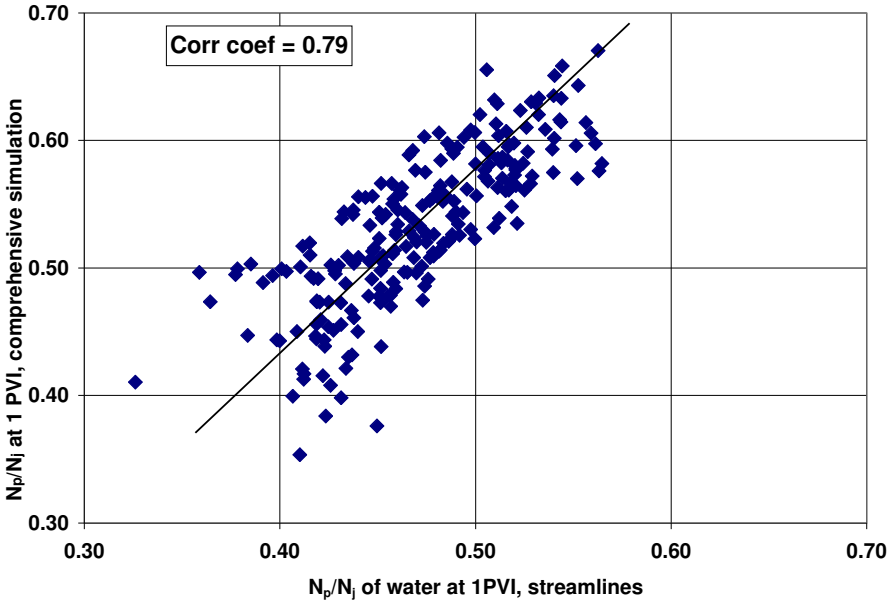

Fig. 5. Correlation among streamline and simulation results for a nonunit mobility ratio displacement. The volume of injected water produced upon the total water injected is plotted at 1 PV.

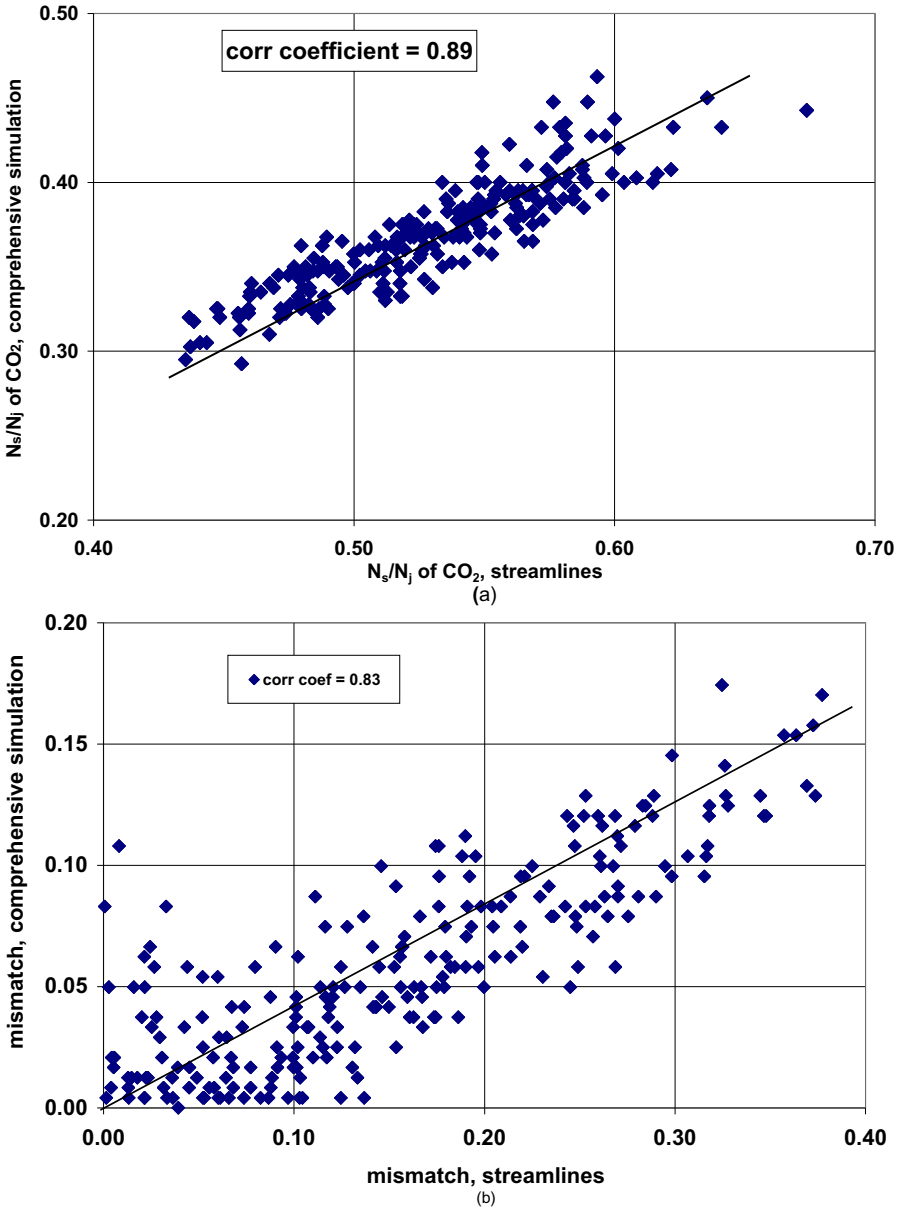

Fig. 6. Correlation among streamline and compositional simulation results for CO_2 injection: (a) the volume of CO_2 stored in the formation upon the total injected and (b) the difference between a realization and the truth case. The elapsed time is 6000 days where 400 x10^6 kg of CO_2 is injected.

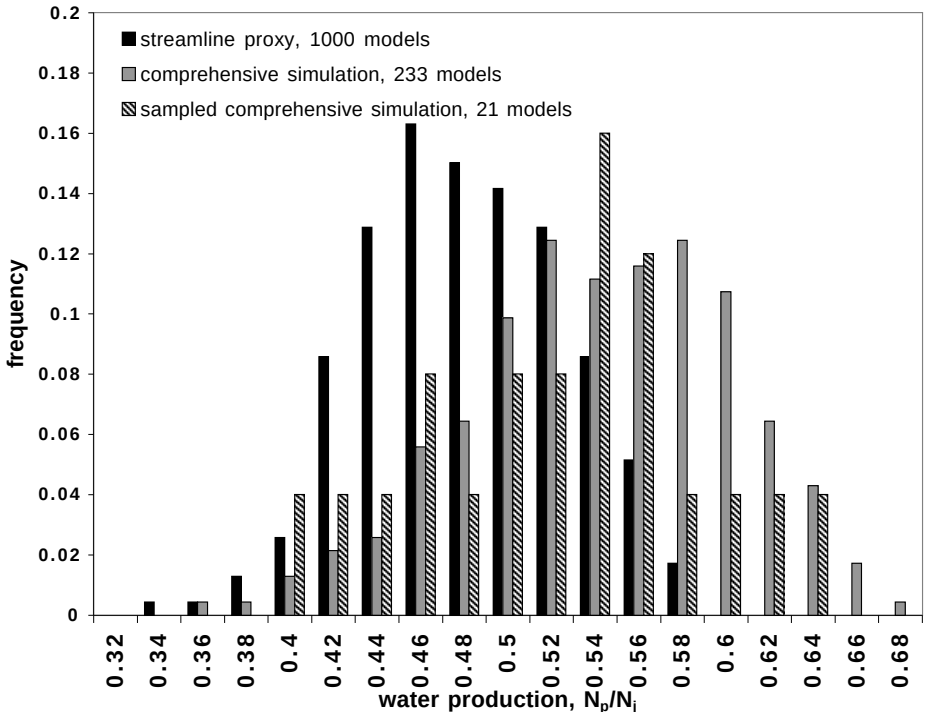

Fig. 7. Histograms of the frequency of water produced upon the total injected at 1 PVI. Distributions obtained (i) using unit-mobility ratio streamlines, (ii) sampling using the streamline based proxy followed by comprehensive reservoir simulation of samples, and (iii) exhaustive simulation of water injection on numerous equiprobable reservoir models.

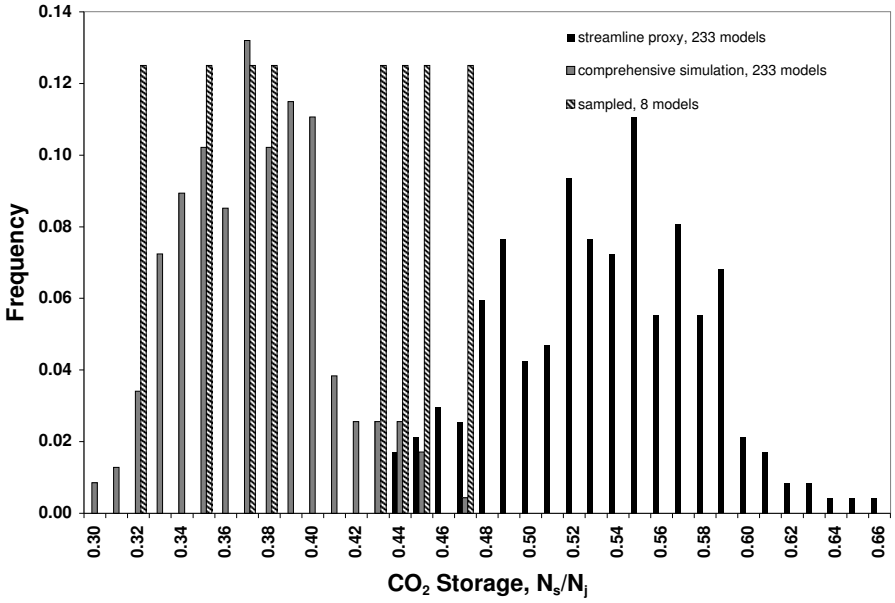

Fig. 8. Histograms of the frequency of CO_2 storage for various reservoir models. The frequency of CO_2 stored upon the total CO_2 injected is plotted at 6000 days where 400 x10^6 kg of CO_2 is injected. Distributions obtained using (i) unit mobility ratio streamlines, (ii) sampling using the streamline based proxy followed by comprehensive reservoir simulation, and (iii) exhaustive simulation of CO_2 injection on numerous equiprobable reservoir models.

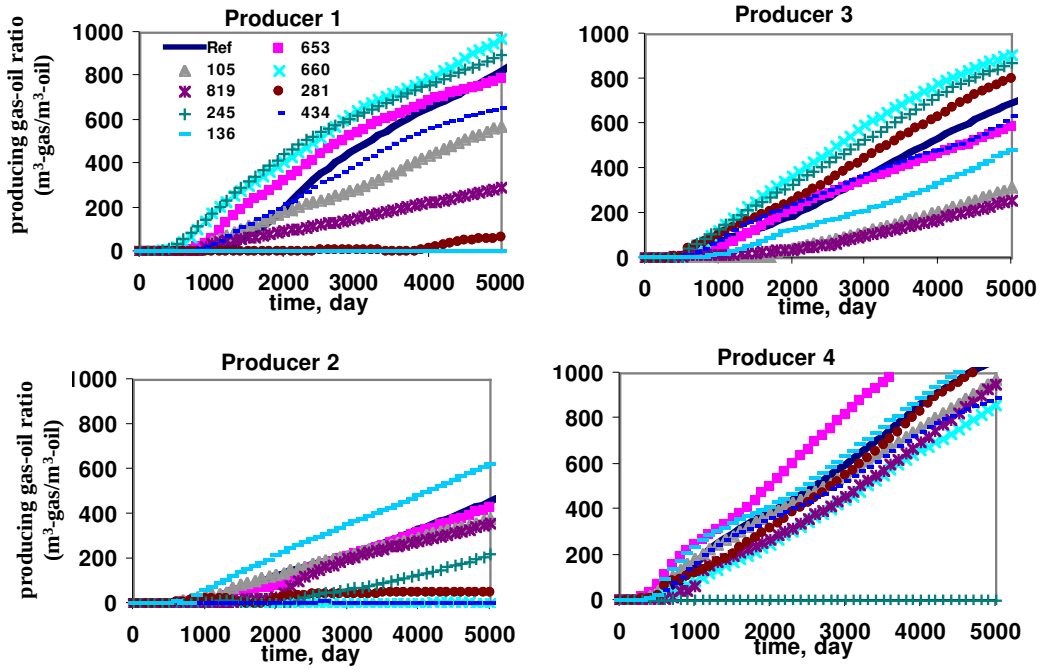

Fig. 9. Producing gas-oil ratio obtained from comprehensive flow simulation of models chosen by the streamline-based proxy.